CHAPTER 2

LITERATURE REVIEW

2.1 Temporal Variability and Spatial Structure of the ITCZ

One of the most striking characteristics of the ITCZ is its variability on a wide range of temporal and spatial scales. The purpose of this section is first to document the characteristic atmospheric time scales with specific reference to interannual, annual, intraseasonal, and diurnal time scales. Second, it is to describe the spatial structure of the ITCZ with respect to convective type, size and intensity, and location.

2.1.1 Interannual Variability

The most important phenomenon in the tropical ocean-atmosphere system at the interannual time scales (period ranging from 2 to 7 years) is referred to as El Niño/Southern Oscillation (ENSO). The oceanic component, the El Niño, is associated with the anomalous warm SST in the eastern-central tropical Pacific Ocean. The atmospheric component, the Southern Oscillation, is referred to the strength of the Walker circulation over the Pacific region, i. e., to the difference in surface pressure between the southeastern tropical Pacific and the Indonesian-Australian regions. According to Trenberth (1997), an El Niño can be said to occur if the 5-running mean of SST anomalies in the Nino 3.4 region (5°N-5°S; 120°-170°W) exceeding ± 0.4°C for 6 months or more. The most commonly used of the Southern Oscillation Index (SOI) is the normalized pressure difference between Tahiti and Darwin. The very strong connection between the El Niño and Southern Oscillation is apparent, when sea surface temperatures

over the eastern-central Pacific Ocean are abnormally warm (El Niño), the Walker circulation weakens or sea pressure drops in Tahiti and rises in Darwin (low SOI). In addition to the quasi-cyclic nature, ENSO exhibits at least two other prominent characteristics, namely irregularities in amplitude and frequency (Wang and Wang 1996) and phase locking with annual cycle (Wyrtki 1975). Table 2.1 shows the El Niño and La Niña events identified using SST anomalies in the Nino 3.4 region and 0.4°C threshold.

Table 2.1. The El Niño and La Niña events identified using SST anomalies in the Nino 3.4 region and exceeding ± 0.4°C threshold.

El Niño events			La Niña events		
Begin	End	Duration	Begin	End	Duration
Aug 1951	Feb 1952	7	Mar 1950	Feb 1951	12
Mar 1953	Nov 1953	9	Jun 1954	Mar 1956	22
Apr 1957	Jan 1958	15	May 1956	Nov 1956	7
Jun 1963	Feb 1964	9	May 1964	Jan 1965	9
May 1965	Jun 1966	14	Jul 1970	Jan 1972	19
Sep 1968	Mar 1970	19	Jun 1973	Jun 1974	13
Apr 1972	Mar 1973	12	Sep 1974	Apr 1976	20
Aug 1976	Mar 1977	8	Sep 1984	Jun 1985	10
Jul 1977	Jan 1978	7	May 1988	Jun 1989	14
Oct 1979	Apr 1980	7	Sep 1995	Mar 1996	7
Apr 1982	Jul 1983	16	Jun 1998	Nov 2000	30
Aug 1986	Feb 1988	19		(predicted)	
Mar 1991	Jul 1992	17			
Feb 1993	Sep 1993	8			
Jun 1994	Mar 1995	10			
Apr 1997	May 1998	14			

Figures 2.1a-b show the Walker circulation during a normal and an El Niño event. During a normal condition (Fig. 2.1a), the trade winds blow towards the west across the tropical Pacific Ocean. These winds pile up warm surface water in the western Pacific, so that the sea surface is about 0.5 meter higher around Indonesia than around Ecuador. The SST is about 8°C warmer in the west, with cool temperature off South America due to an upwelling of cold water from deeper levels. The thermocline, which marks the boundary between warm surface and cold deep water, is tilted. It reaches almost up to the sea surface in the eastern equatorial Pacific. Rainfall is found in the rising branch of Walker circulation over the warmest water, whereas the eastern Pacific is relatively dry.

During an El Niño event (Fig. 2.1b), the trade winds relax in the central and western Pacific leading to a depression of the thermocline in the eastern Pacific, and an elevation of the thermocline in the western Pacific. The result is a rise in SST in the eastern Pacific. Rainfall follows the warm water eastward, associated with flooding in Peru and drought in Indonesia. The eastward displacement of the atmospheric heat source overlaying in the warmest water results in large changes in global atmospheric circulation, which in turn force changes in weather in regions far removed from the tropical Pacific. The mature phase of ENSO tends to occur in boreal winter and lasts for several months to one year.

The equatorial Pacific is especially sensitive to temperature perturbations because SST exceeds 2.5°C there. The exponential dependence in the Clausius-Clapeyron equation then implies that small variations of SST produce large changes in evaporation and latent heat transfer. The relaxation of the trade winds during an ENSO event results

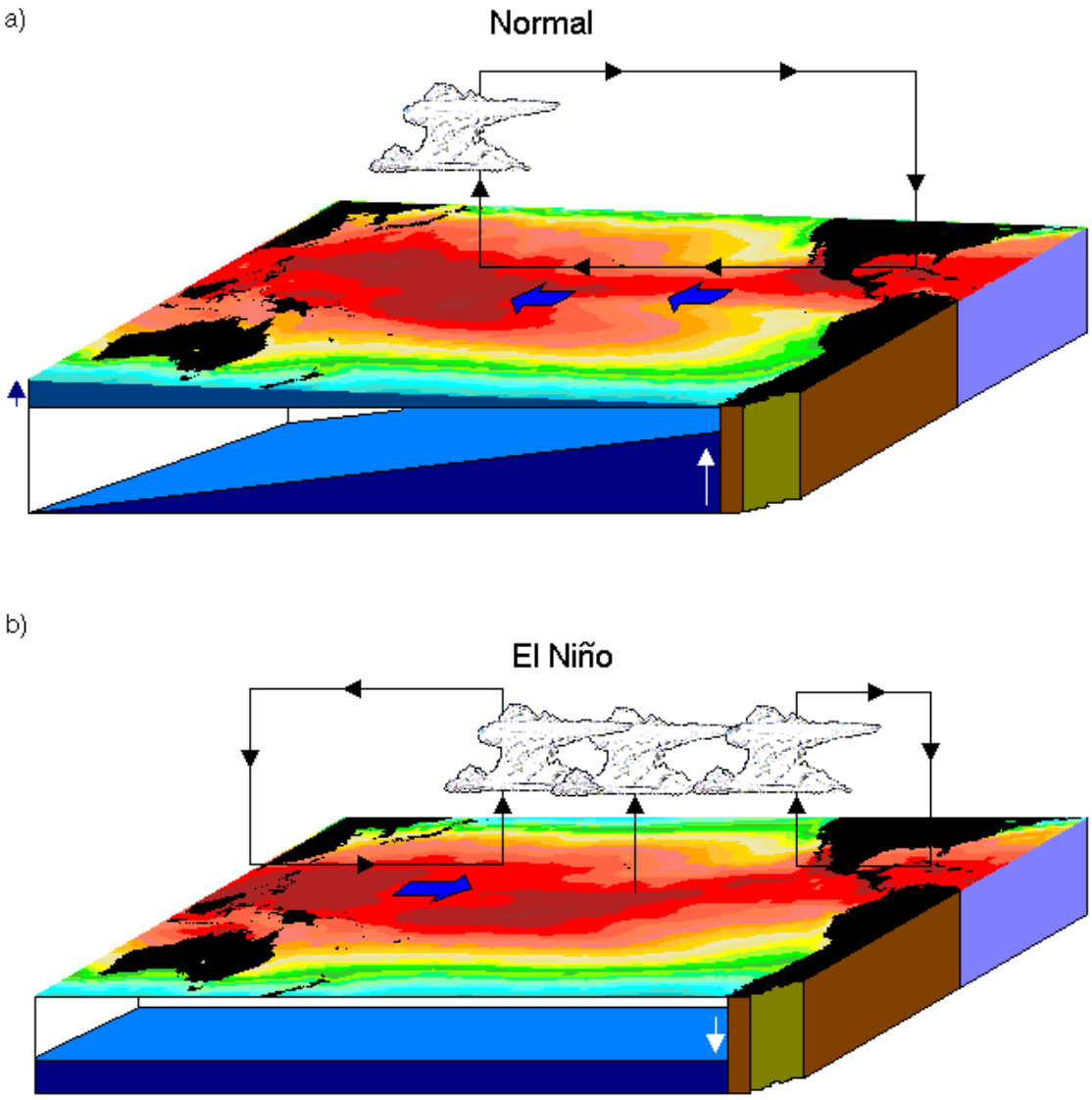

Figure 2.1. The Walker circulation over the Pacific Ocean during a) a normal condition and b) an El Niño event.

in the stress that kept warm water piled up against the western boundary is reduced, causing this water mass to spread out. Because of the equatorial wave guide, the outflow proceeds eastward along the equator in the form of an equatorial Kelvin waves (Gill 1982). This process tends to flatten the east-west surface slope, and it transports heat

from west to east. At the eastern boundary, the Kelvin waves are partly reflected as slowly westward moving equatorial Rossby wave.

The ENSO events have resulted in the devastating consequences on climate for more than half of the globe. As illustrated in Fig. 2.2, Ropelewski and Halpert (1987, 1988) showed that ENSO is often related to heavy rainfall in the central and eastern Pacific regions, but to drought in the surrounding anvil that covers Indonesia, the Philippines, Thailand, Hawaii, and eastern Australia. In the western part of South America, the equatorward displacement of the ITCZ brings heavy rainfall to Ecuador and northern Peru, but drought to parts of Bolivia and central America. In the Indian sector, there is a strong tendency for monsoon to fail. Southeastern Africa tends to suffer drought, while equatorial east Africa increases rainfall. In North America, greater than normal precipitation occurs in the Great Basin and Gulf of Mexico. The sign of these changes is generally reversed during cold La Niña events.

It is known that the 1982/83 and 1997/98 ENSO events are the strongest events in the century. Bell and Halpern (1998) found that in absolute terms, the magnitude of the warming SST in the eastern-central Pacific during the 1997/98 ENSO was at least as large as the 1982/83 ENSO event. However, the 1997/98 ENSO was unique in the rapidity with which it grew. Accompanying the 1997/98 Pacific warming have been the usual ancillary climate variations associated with ENSO, namely drought over Indonesia, the western Pacific, and East Asia, and significant flooding around the eastern Pacific. However, despite the magnitude of the 1997/98 ENSO, there were a number of ancillary climate variations that were very different from other strong ENSO years. Instead of drought over Australia, the rains were normal or slightly below average. The Indian

monsoon, which is often weak during an ENSO, was essentially normal. Precipitation in East Africa, usually slightly enhanced during an ENSO, was perhaps the heaviest in this century and resulted in massive flooding. Most of the differences that have occurred between the 1997/98 ENSO and others have occurred around the Indian Ocean region.

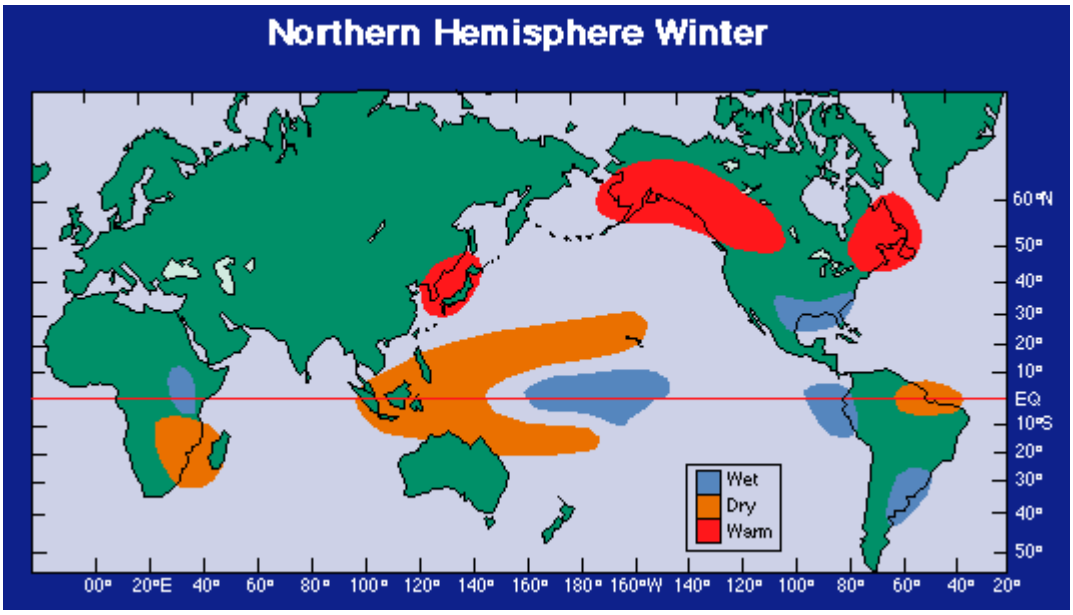

Figure 2.2. Precipitation anomalies during typical El Niño events during Northern Hemisphere winter.

Many ENSO prediction models have been developed over the last 20 years. Barnston et al. (1994) classified these models into three groups: dynamical-coupled models, hybrid-coupled models, and statistical models. The dynamical-coupled models include intermediate coupled models for both ocean and atmosphere (Zebiak and Cane 1987) and an ocean general circulation model (GCM) coupled with an atmospheric GCM (Ji et al. 1994). The hybrid-coupled models include ocean GCM coupled with a statistical

atmosphere (Neelin 1990; Barnett et al. 1993). The statistical models include canonical correlation analysis (Barnston and Ropelewski 1992) and constructed analog model using an optimal linear combination (Van den Dool 1994). With increasing physical understanding, dynamically based forecasts have the potential to become more skillful than purely statistical ones. Currently, however, the predictive skills achieved by the dynamical and hybrid models are approximated with statistical models at a lead time of 6 months.

Over Indonesia, the ENSO-related drought conditions often result in large-scale forest fires particularly over Sumatera and Kalimantan islands (Malingreau et al. 1985; Wooster et al. 1998). As in many countries in the tropics, a 'burning season' occurs every year in Indonesia, primarily to prepare agricultural lands for plantation and as a 'slash and burn' practice at the forest edge in order to extend the area available for agriculture before the rains. These burning activities become out of control during long drought conditions. The 1997/98 ENSO event was one of the largest events on record. It was reported that 3 million hectares of the forest were burned in Kalimantan and 1.5 million hectares in Sumatera. It is known that haze from tropical burning contains large concentrations of carbon monoxide, carbon dioxide, nitrogen monoxide, and ozone. Smokes from the forest fires initially rises to a few kilometers, convective activity ultimately mixes materials from the haze layers down into the boundary layer forming a ground level smog. As a result, the smokes that blanketed the neighboring countries of Malaysia, Singapore and Brunei from September 1997 to April 1998 had substantial effects on human beings such as reduced visibility in the regions, aggravated health conditions, and airport and schools closures.

2.1.2 Annual Variability

On the annual time scales, the ITCZ moves in association with the zone of maximum seasonal temperatures. Figures 2.3a-f show the annual cycle of convection over the global tropics as obtained from the 17-year mean highly reflective clouds (HRC) data (Hastenrath 1990). In general, the ITCZ marches south in the Northern Hemisphere fall and winter and north in the Northern Hemisphere spring and summer. The mean position of the ITCZ reaches its farthest south position at most longitudes in January-February (Fig. 2.3a). The convection band moves gradually northward in March-April (Fig. 2.3b) and May-June (Fig. 2.3c) and reaches its northernmost position in July-August (Fig. 2.3d). In September-October (Fig. 2.3e) and November-December (Fig. 2.3f), the convection belt moves southward. The main feature to note is the migration of the ITCZ which is largest over the continent areas, the Indian and western Pacific oceans, but relatively small across the eastern Pacific and Atlantic oceans. In addition, from both the south American and Indonesian convection centers, a band of abundant cloudiness extends southeastward reflecting the South Atlantic Convergence Zone (SACZ) and South Pacific Convergence Zone (SPCZ), respectively. While the SPCZ persists all year, the SACZ is well developed only during the Northern Hemisphere winter.

Over a large portion of Asia, parts of Africa (Sahel), and northern Australia, the annual cycle of convection is dominated by the Asian-Australian (AA) monsoon that implies a complete reversal of wind regimes in the course of the year (Fig. 2.4a-b). Nowhere else in the globe is the annual reversal of wind and rainfall regimes as spectacular as over these regions. The AA monsoon is one of key components of the earth's climate system affecting the livelihood of more than 60% of the population over

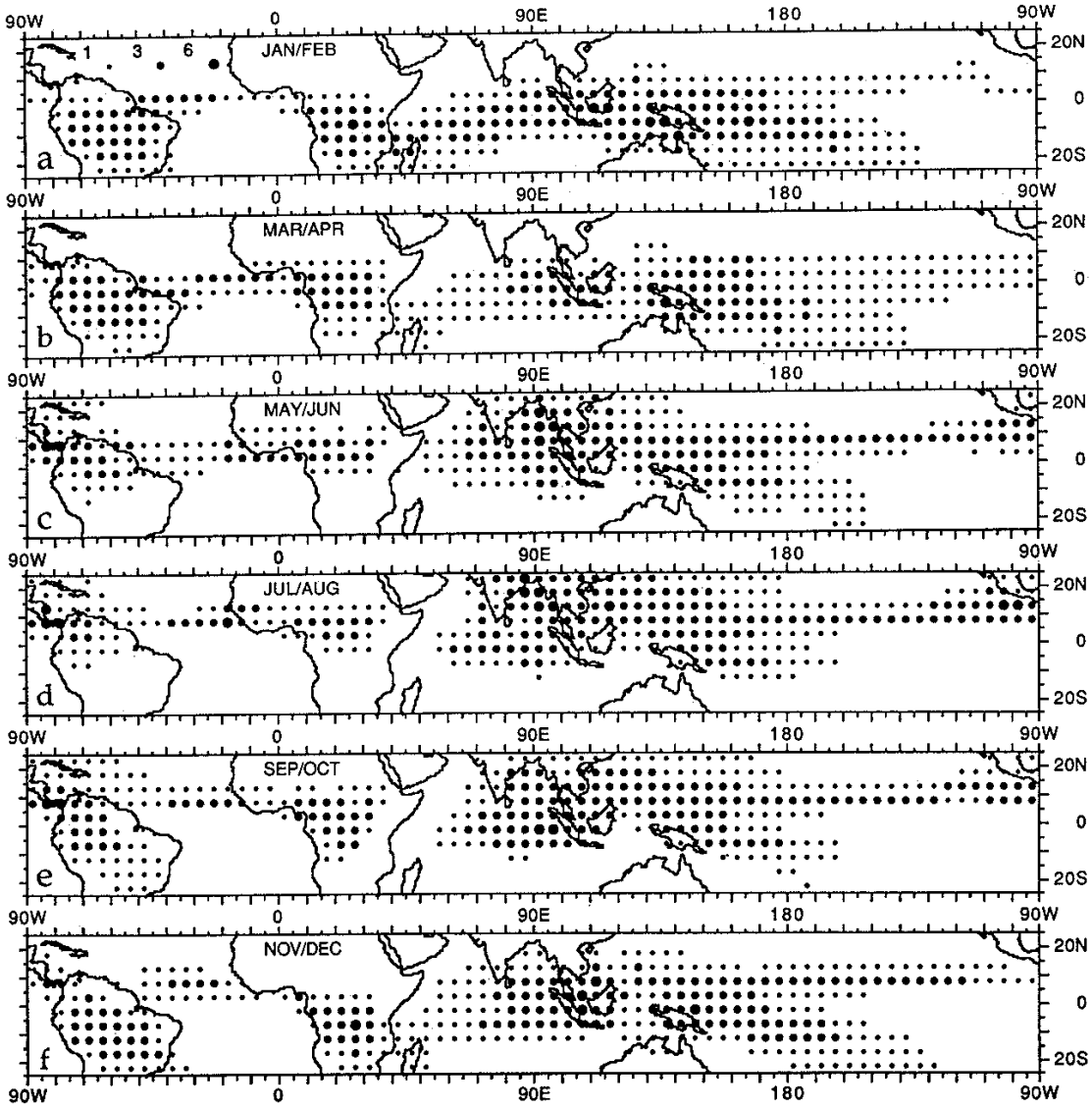

Figure 2.3. The mean annual cycle of HRC patterns (from 1971 to 1987). a) January-February, b) March-April, c) May-June, d) July-August, e) September-October, f) November-December. Dots of varying size denote average number of days with HRC per month, for classes HRC < 1 (blank), 1 ≤ HRC < 3, 3 ≤ HRC < 6, HRC ≥ 6, as indicated in legend in panel a). Adapted from Hastenrath (1990).

the tropics (*World Bank Atlas*, 1992). There are three main driving mechanisms of the planetary scale AA monsoon. The first mechanism is the differential heating between the lands and the ocean and the resultant longitudinal anomaly in the zonally symmetric heating gradient of the annual cycle. The second mechanism is the impact of planetary earth's rotation (Coriolis force) which produces latitudinal character into the dynamic response of the atmosphere to the differential heating perturbations. The third mechanism is moisture processes in the atmosphere which raise land-ocean pressure differences.

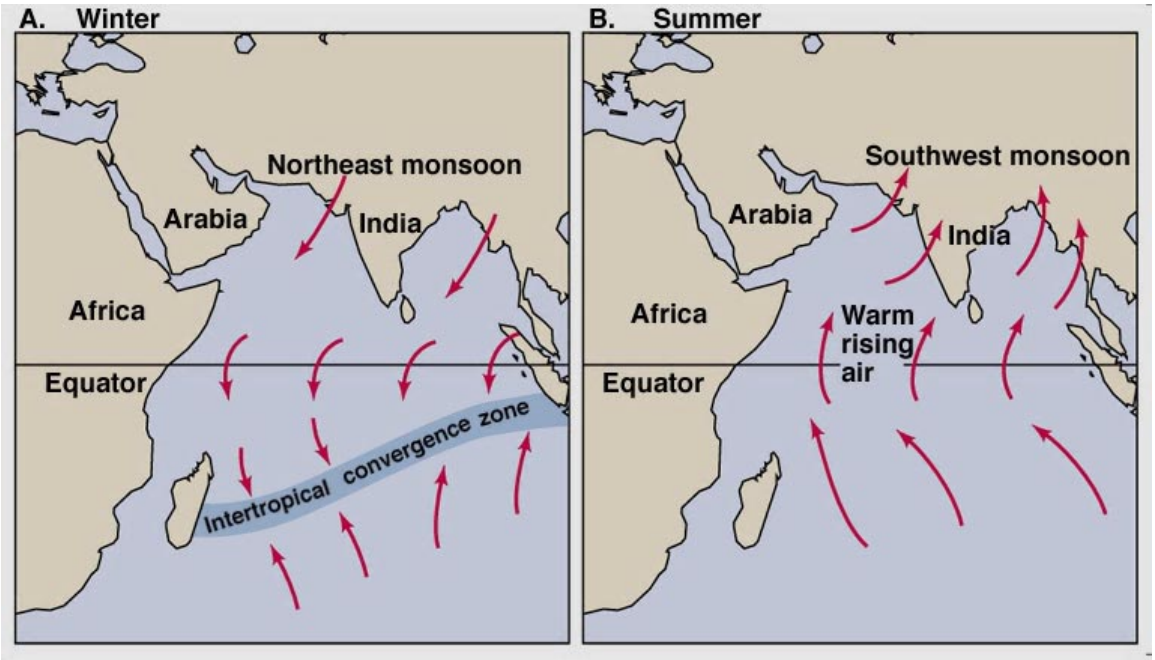

Figure 2.4. Primary synoptic-scale circulation of the Asian-Australian monsoon during a) winter and b) summer seasons.

The northeast (winter) monsoon (Fig. 2.4a), which dominates the general circulation from November to February, is characterized by northeasterly trade winds over the western Pacific and Southeast Asia from about 20°N to the equator. Proceeding southward across the equator, the low-level flow turns to westerly winds which extend between 10°S and 20S° across Java, northern Australia, and the southwest Pacific. During the northeast monsoon, the main heating source is located over northeast Australia and the equatorial western Pacific, while the cooling source is centered over the Asian Continent. Heavy rainfall and associated heat release of condensation exist between 5°S and 15°S extending from the Indian Ocean to the western Pacific Ocean.

The southwest (summer) monsoon (Fig. 2.4b), which prevails from June to September, is a continuation of the southwesterly winds from southern Indian Ocean to Asia. During the southwest monsoon, the primary region of heating is situated over the Tibetan Plateau and cooling region over the Southern Indian Ocean. Following the onset of the monsoon, there is an intense low-level jet along the east coast of Africa and over the Arabian Sea (the Somali Jet). Significant fluxes of moisture from the ocean surface to the atmosphere occur over these regions, which fuel the deep convection rains over India and neighboring countries. Heavy precipitation also occurs over southern and central China. However, its moisture source appears to be primarily from the equatorial regions of Indonesia.

Although a large number of studies have been made for the southwest monsoon episode (Krishamurti et al. 1985; Parasnis 1991; Bhaskaran et al. 1998; Arpe et al. 1998; Annamalai et al. 1999), similar studies for the northeast monsoon have been somewhat limited (Lau and Li 1984; Dudhia 1989; Kitoh 1992; Krishnamurti et al. 1993; Tomita

and Yasunari 1996). The northeast monsoon plays an important role not only for regional climate in South East Asia and Australia regions, but also for the extratropical teleconnection associated with various spatial and temporal scales. The northeast monsoon exhibits distinct characteristics that differ considerably from being a mere mirror image to its southwest counterpart. The basic differences among other things arise from the fact that during the northeast monsoon the major convection is over the maritime continent (part ocean part land) and the main heat source is located over the equatorial belt where the divergent component is more prominent (Lau and Chang 1987).

Similar to the southwest monsoon, the northeast monsoon is also characterized by active and break periods. The first occurrence of mean low-level westerly winds between the equator and 10°S defines the onset, and strengthening (weakening) of the winds indicate active (break) periods in the monsoon (Hendon et al. 1989). Puri (1994) carried out a study to access the performance of the Bureau of Meteorology Research Centre (BMRC) global spectral model in simulating various features of the summer monsoon during the Australian Monsoon Experiment (AMEX). Two time scales were considered: short-range (< 5 days) and long-range (30-40 days). Over both time scales, the model was able to simulate most of the features of the monsoon such as onset, mean circulation, and the active and break periods. Over the short-range simulation, the prediction of monsoon was sensitive to initial conditions, particularly the moisture field, and to the parameterization of cumulus convection. Over the long-range simulation, it was shown that the mean circulation and precipitation were sensitive to SST.

2.1.3 Intraseasonal Variability

On the intraseasonal time scales, the migrations of the ITCZ are dominated by the 40-50 day Madden-Julian oscillation (Madden and Julian 1971, 1972). Its spectral signature in zonal wind and surface pressure is concentrated around 40-50 day period, while that in convection is much broader (i. e., 35-95 days). Convection anomalies are confined to the Indian and western Pacific oceans, while wind perturbations tend to propagate around the equator. In addition to the eastward movement of the system, individual cloud clusters propagate westward (Nakazawa 1988). In general, the strongest eastward propagating anomalies of convection and circulation occur during December to April. The local zonal scale of the convective activity over the Indian Ocean and western Pacific oceans is about 7500 km such that while enhanced convection covers the Indian ocean, suppressed convection covers the western Pacific. A half cycle later, when the enhanced convection has propagated into the eastern Pacific, the reverse occurs.

Some conceptual models of intraseasonal oscillation have suggested a strong influence of equatorial convective systems on local changes of SST. Figure 2.5a-c show three models of intraseasonal oscillation based on wave-CISK (Conditional Instability of the Second Kind) theory (Lau et al. 1989), wind-induced surface heat exchange (WISHE) theory (Emanual 1987), and the air-sea convective intraseasonal interaction (ASCII) theory (Flatau et al. 1997), respectively. According to the wave-CISK theory (Fig. 2.5a), the region of convergence between easterlies and westerlies in an eastward propagating Kelvin wave (region C) becomes the preferred site for the subsequent development of convection. The formation of the new cells in this region causes the eastward propagation

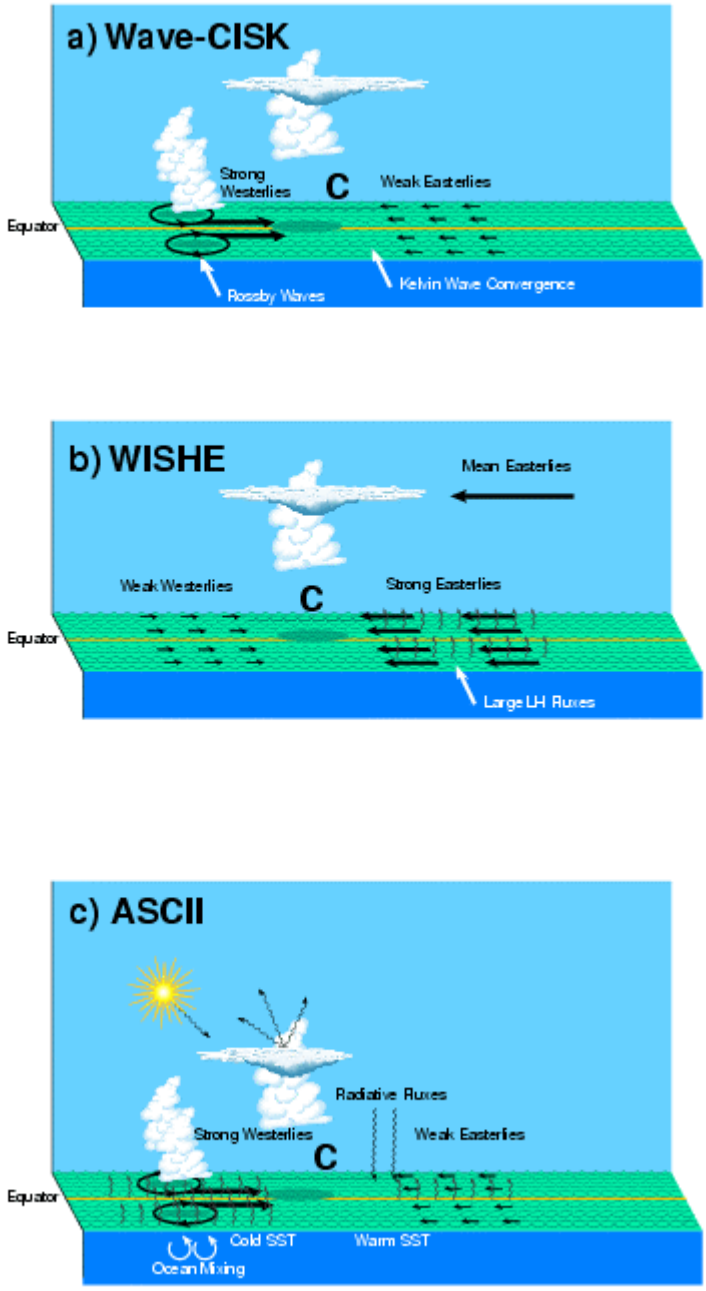

Figure 2.5. Schematic diagrams of three conceptual models of intraseasonal oscillation. a) Wave-CISK, b) wind-induced surface heat exchange (WISHE), c) air-sea convective intraseasonal interaction (ASCII). Adapted from Flatau et al. (1997).

of the equatorial super cluster, while the individual clusters that form on both sides of the equator move west as Rossby waves. According to the WISHE theory (Fig. 2.5b), in the presence of the mean equatorial easterly wind, enhanced surface evaporation in the region of the strong easterlies can provide surface forcing necessary for development of instabilities similar of observed oscillations. Increased surface fluxes in the region of large easterlies are responsible for positive temperature perturbations that cause the eastward propagation of the wave and provide energy for growth of instability. However, the assumption of mean easterly flow is not always true, especially during the ENSO years. According to the ASCII theory (Fig. 2.5c), the surface forcing necessary for enhancement of the Kelvin wave is provided by the SST distribution generated by the super cluster itself. The SST decreases under and west of a convective source. This SST drop is due to the cloud shield effect, ocean mixing, and evaporative fluxes associated with strong equatorial westerly winds. East of the convective source, in the region of weak winds associated with the convergent region of an easterly propagating Kelvin wave, SST can increase. This zonal SST gradient causes zonal changes in surface moist static energy and provides surface forcing, promoting development of convection in convergent regions.

2.1.4 Diurnal Variation

On day-to-day basis, the weather in the tropics is dominated by the local to mesoscale diurnal variations of the cumulus convective activity or rainfall and surface wind circulations. The diurnal variation of rainfall over the tropics is much more regular than that over the mid-latitudes. Apart from the infrequency of fronts, the prevalence of

diurnal processes in the tropical troposphere is the reason for this difference (Nieuwolt 1977).

Two main types of diurnal rainfall regime can be recognized in the tropics. First, the inland type which displays a maximum of rainfall during late morning or afternoon. The main reason for this distribution is convection caused by surface heating of the land. Second, the marine or coastal type which shows a maximum of rainfall during night or early hours of the morning. This regime is caused by nighttime 'convection' which the upper troposphere is cooled by radiation loses, while the lower layers remain warm by close contact with the surface water. However, it is argued that these diurnal cycles are much more complicated than this simple picture. Local factors, which have a strong effect on small-scale processes involved in diurnal rainfall distribution, are the main reason for the many deviations from the ideal type. Over lands, the local variations in the diurnal regimes are caused by topography, vegetation type, soil humidity, and sea breeze. Over the coastal area, local factors influencing the diurnal rainfall distribution are land breeze, the form of the coastline, the topography of the coastal areas, the presence of swamps, lakes, rivers, or irrigated fields (Nieuwolt 1977).

The diurnal variability in tropical rainfall has been investigated and documented for a variety of purposes using different data sources. Murakami (1983) examined diurnal cycle in the Asian monsoon regions using the satellite infrared data. The results showed that the suppressed convective activity over the lands is found in the morning hours with the minimum around 0900 LST and maximum enhancement around 1800 LST. In contrast, the enhancement of the convective clouds over the oceanic areas occurs around 0600-0900 LST and the suppressed convection between 1800 and 2100 LST.

Slingo et al. (1987) used OLR data with an atmosphere GCM to simulate the diurnal cycle of the tropical convection. They found the largest mean diurnal variations are in the Indian Ocean, Indonesia, and in the Pacific Ocean extending from 150°E across the dateline to 150°W. It is then suggested that the cloud diurnal variations should be accounted for in climate models for better understanding the origin of the observed variations.

Janowiak et al. (1994) determined results of an analysis of the diurnal cycle in oceanic tropical rainfall using satellite and in situ data. The deep convection with cloud top temperatures < 215K in the tropics is most frequently observed over land between 1800 and 2100 LST. Over the oceans, the convection is found to occur much earlier in the day with a peak between 0000 and 0800 LST.

Chang et al. (1995) examined the diurnal variation of oceanic rainfall from the Defense Meteorological Satellite (DMS) Spectral Sensor Microwave/Imager (SSM/I). The most frequent rain period over the Indian, Atlantic, and Pacific oceans is in early morning between 0000 and 0600 LST over the ITCZ regime. The areas in which evening rain is larger than morning rain are mostly located in regions where the rain total is small, such as the southern Pacific and Atlantic dry zone.

The diurnal variations of the surface wind field over the tropical Pacific Ocean are studied among others by Deser and Smith (1998) using the Tropical Atmosphere-Ocean (TAO) array data. They found that the diurnal variations account for 82% of the mean daily variance of the meridional wind component. The diurnal cycle of the meridional wind field exhibits a pronounced zonally symmetric component with opposite phase on either side of the equator. The southerly winds reach a maximum at the north of the

equator in the morning between 0600 and 0900 LST, but at south of the equator in early evening between 1800 and 2000 LST. In addition to the zonally symmetric component, there are east-west differences in the structure of the diurnal meridional winds. The diurnal cycle at the equator is large in the eastern Pacific and negligible in the western Pacific. Moreover, the diurnal cycle of the equatorial wind divergence changes seasonally in the eastern Pacific and interannually in the western Pacific in proportion to the strength of the mean divergence.

2.1.5 Spatial Structure of the ITCZ

The differences in the amplitude and phase of the ITCZ excursions at different longitudes emphasize the different atmosphere and surface forcing regimes. Clouds in the tropics occur in a spectrum of sizes ranging from small isolated non-precipitating cumulus to large 'cloud clusters' with a scale of 100-500 km and containing both deep convective cells and stratiform precipitation (Houze and Betts 1981).

Williams and Houze (1987) studied the daily cloud clusters observed during the Winter Monsoon Experiment (MONEX) which was conducted in the region of the Kalimantan in December 1978. They found that the difference in the size distributions of large cloud clusters between land and sea was considerable. Over the sea a substantial proportion of the cloud cover, and hence the rainfall, comes from clusters with maximum areas greater than 1.2×10^5 km^2, whereas no clusters are observed in this size category at all over the land (the maximum size is about 6×10^4 km^2). In addition, large clusters tend to develop over the land during the evening period and over the sea during the morning period.

A hierarchy structure of cloud clusters within the intraseasonal variations over the western Pacific Ocean has been studied by Nakazawa (1988). He found that a zonal wave number 1 structure with a period range from 30 to 60 days moves eastward. Embedded with this planetary-scale convection are super clusters. A super cluster consists of 2 or 3 cloud clusters several hundred kilometers wide with 1-2 day life scale moves eastward with a phase speed of about 10 ms^{-1} to 15 ms^{-1}. Although each cloud cluster moves westward, a super cluster moves eastward due to the successive formation of a new cloud cluster east of the mature stage cloud cluster. He also found that during the onset phase of the 1986/87 ENSO event, an eastward moving super cluster was observed over the western Pacific to the dateline.

Basic details of the size and intensity of tropical convection are given by Mohr and Zipser (1996). They found that over tropical oceans and continents no significant relationship occurred between the size and intensity for the mesoscale convective systems (MCSs) defined as an area below 250K of at least 2000 km^2, with an enclosed minimum brightness below 225K. In their study, tropical South America, Africa, and the warm pool had the greatest number of MCS. Moreover, the MCSs are 35% more frequent over the oceans at sunrise than at sunset and 60% more frequent over continents at sunset than at sunrise. In general, the MCSs tend to be larger at sunrise than at sunset. In the subsequent study, Mohr et al. (1999) described the fact that although MCSs constituted 10-20% of the regional populations, they contributed 70%-80% of the rainfall. Central America, Southeast Asia/India, the Congo, and Sub-Saharan Africa had distributions significantly more intense than the oceanic regions. The continent regions have the largest number of intense MCSs with a peak at 175K, while the oceanic regions at 200K.

On the monthly average, the spatial structure of the ITCZ over the eastern Pacific and Atlantic oceans is characterized by a narrow well-defined cloud, which reflects the convergence of surface air from the two hemispheres, and located north of the equator. In contrast, over the Indian and western Pacific oceans the ITCZ is characterized by a relatively broad cloud band. Philander et al. (1996) showed that the ocean-atmosphere interactions are most effective where the thermocline is shallow, because the winds can readily affect SSTs in such regions. The thermocline happens to shoal in the eastern equatorial Pacific and Atlantic oceans, because the easterly trades winds prevail over these regions. On the other hand, the influence of continents is so profound in the Indian and western Pacific oceans as mentioned in Section 2.1.2, where the cross-equatorial monsoons are more prominent than the easterly trade winds. Over the land, the mean cloud cover expands due to the additional influence of surface heating, topography, albedo, soil moisture, and by the geometries of the continents.

2.2 Large-Scale Tropical Air-Sea Interactions

The largest part of the tropics is occupied by oceans, i. e., the tropical Pacific, Atlantic, and Indian oceans. Therefore, the large-scale dynamics of the tropical oceans and atmosphere is closely related. Energy is transferred from the atmosphere to the ocean surface mixed layer driving the circulation of the upper ocean. In turn, energy from the ocean is fed back to the atmosphere affecting the atmosphere circulation, the weather and the climate.

Many studies have shown that convection in the tropics are closely associated with SST. The annual cycle in SST in the eastern Pacific Ocean exhibits many

similarities with annual cycle of rainfall (Horel 1982). Shukla and Wallace (1983) found during the mature phase of the ENSO event an eastward shift of the belt of heavy convective precipitation in the western Pacific Ocean is associated with positive SST anomalies in the eastern Pacific.

Some evidences that a certain SST range produces convection are given by previous investigators. Gadgil et al. (1984) found that over the Indian Ocean deep convection increases linearly with SST in range of 24.5°C < SST ≤ 28°C, whereas SST > 28°C no apparent relation between SST and deep convection could be found. Gutzler and Wood (1990) also showed that over the tropical Pacific Ocean the linear correlation between SST and Outgoing Longwave Radiation (OLR) is statistically significant only in limited areas with SST near 27.5°C but not in region with SST > 28°C.

Waliser and Graham (1993) used the statistical analysis of the relationship between SST, OLR, and HRC to infer the role of convection in limiting ocean surface temperatures. They showed that the intensity of organized convection rises sharply as SSTs increase from 26.5°C to 29.0°C, reaches a maximum at 29.5°C, and then declines at higher temperatures. The presence of organized convection tends to limit upward excursions of SSTs. On the basis of a 'thermostat' hypothesis of SSTs being limited by the solar shielding effects of thick cirrus clouds and observed values of radiative feedback, Ramanathan and Collins (1991) calculated upper limits on SST of about 29°C-32°C.

Zhang (1993) found that tropical deep convection remains weak and rarely observed for SST < 26°C, the frequency and mean intensity of deep convection

substantially increase with SST from 26°C up to about 29.5°C-30°C, and then decay for further increasing SST. Meanwhile, in the warm pool region with SST > 27°C, situation with no deep convection and vigorous deep convection can both be observed. In his study, there is no evidence of a 'critical SST' as suggested by Gadgil et al. (1984) and Waliser and Graham (1993). The increase in deep convection with SST is smooth and continuous and no distinct change in deep convection occurs at any particular SST.

However, the above results appear to contradict other studies that suggest convection anomalies are primarily associated with anomalous low-level moisture convergence rather than anomalies in evaporation. Carnejo-Garrido and Stones (1977) showed that over the tropical Pacific Ocean near 10°S in the region where condensation heating is a maximum, the evaporation and atmosphere heating by the surface are a minimum. This implies that the region of enhanced condensation is associated with a region of moisture convergence rather than with a region of enhanced evaporation, and that the SST gradients only play a secondary role in forcing the Walker circulation.

Although it is frequently assumed that the flow generated by the latent heat release in cumulus towers is an important component of the low-level convergence, Lindzen and Nigam (1987) argued that SST along with its gradients is a major contributor to the low-level tropical flow and convergence. These SST gradients are communicated to the atmospheric boundary layer by turbulent exchange from the surface, giving rise to low-level density gradients, and thus to low-level pressure gradients. These pressure gradients force the low-level tropical wind field and thus help determine the distribution of deep convection and rainfall.

Graham and Barnett (1987) found that over the Indian and Pacific oceans, SSTs in excess of 27.5°C are required for large-scale convection to occur. However, SSTs above 27.5°C are not a sufficient condition for convection and further increases in SST appear to have little effect on the intensity of convection. In addition, when SSTs are above 27.5°C, surface wind divergence is closely associated with the presence and absence of deep convection.

Lau et al. (1997) computed the influence of the large-scale atmospheric circulation on the relationship between SST and tropical convection inferred from OLR. They found that under subsidence and clear sky conditions, there is an increase in OLR with respect to SST at a rate of 1.8-2.5 $Wm^{-2}(°C)^{-1}$. In region of large-scale ascending motion, the rate of OLR reduction is found to be a strong function of the large-scale motion field. An intrinsic OLR sensitivity to SST is found approximately -5 to -4 $Wm^{-2}(°C)^{-1}$ in SST range of 27°C-28°C under condition of weak large-scale circulation, but under the influence of strong ascending motion the rate can be increased from -15 to -12 $Wm^{-2}(°C)^{-1}$ for the same SST range. On the other hand, deep convection and large-scale circulation exhibit a nearly linear relationship that is less dependent on SST and geographic locations.

2.3 Predictability of Climate Variability over Indonesia and the Indian Ocean

It has been suggested that weather and climate predictions should be more feasible for the tropics, because their variability in the lower latitudes is in large part due to slowly varying anomalies at the lower boundary of the atmosphere such as SST, soil moisture,

etc. (Charney and Shukla 1981). However, examination of research and operational climate predictions show at best only a marginal level of skill. This suggests that long-range prediction may be feasible only for certain selected areas, elements, and seasons (van den Dool and Saha 1990). The Indonesian region and the Indian Ocean appear to be such regions. This section examines the evidence for climate predictability in these regions and discusses the possible physical mechanisms involved.

2.3.1 Over Indonesia

The combination of latent heat release from the ocean and sensible heat release from the lands makes the maritime continent of Indonesia (Fig. 2.6) favorable for convection all year round. However, in general the rain activity tends to be concentrated during the northeast monsoon from November to February. This is the season where a quasi-permanent low-pressure center is best developed and low-level convergence is pronounced. The relationship between the Southern Oscillation and rainfall over Indonesia has been recognized by Dutch meteorologists since the early years of the twentieth century (Braak 1919; Berlage 1927; de Boer 1947; de Boer and Euwe 1949a,b; Schmidt - ten Hoopen and Schmidt 1951; Resnick 1952) as reviewed by Hastenrath (1991).

Building on the previous studies of Braak (1919), Berlage (1927), and Resnick (1952), Nicholls (1981) presented evidence that early wet season in Indonesia can be successfully predicted from prior observations of atmospheric pressure over northern Australia. This predictability was based on general continuity in the spatial distribution of correlations between June-August pressure in Darwin and September-November rainfall

Figure 2.6. Map of Indonesia and neighboring countries.

Indonesia using data from 1883-1940. Statistically significant correlations existed over the central and eastern parts of the region with the largest magnitude occurring around the Banda Sea.

Nicholls (1982) constructed a linear single-parameter regression model of September-November rainfall in Jakarta versus August pressure in Darwin during 1951-69. He then used this relationship to predict September-November rainfall during each of the years from 1970 to 1980. For this independent data set he succeeded in predicting 44% of the interannual rainfall variance. A later experiment (Hastenrath 1987) examined the predictability of monsoon rainfall over Java for the period 1961-83 based on pressure data in Darwin from 1911 to 1983. It is found that pressure persistence, i. e., the

concurrent correlation of pressure and rainfall, and the predictability of rainfall from antecedent pressure are all strongest in June-November and weakest in December-May. Considering the hydrostatic effects which cold/warm surface waters favor high/low pressure, these serve to explain the strong persistence during the summer monsoon as compared to the winter monsoon.

Hachert and Hastenrath (1986) examined the mechanisms of rainfall anomalies over Java using the ship observation in the Indian Ocean (30°N-30°S; 30°E-120°E) from 1911 to 1973. Between December and January, anomalously high pressure near Southeast Asia along with anomalously low-pressure over Indonesia entail an enhanced meridional pressure gradient, northeasterly flows over the South China Sea and Bay of Bengal, and enhanced northwesterly flows over the Indonesian waters. The increased northerly wind component to the north and intensified westerlies over the equatorial Indian Ocean result in enhanced convergence and cloudiness over Java, while surface waters are cold.

The relationship between ENSO and rainfall over Indonesia has been investigated by Quinn et al. (1978). They pointed out that drought during the dry season of easterly surface winds in May-November usually coincided with El Niño events. Meanwhile, the coincidence of winter monsoon drought and El Niño years has been identified by Rasmusson and Carpenter (1982). More recent studies of Ropelewski and Halpert (1987) demonstrated that 80% of the ENSO events from 1879 to 1982 were accompanied by below normal rainfall in Indonesia between June and November. Moreover, Ropelewski and Halpert (1989) found that 90% of La Niña events were associated with abnormally wet season over Indonesia between July and December.

The relationship between ENSO and SST in the Indonesian region was first studied by Nicholls (1984). The SST anomalies over the Indonesian waters show strong persistence approximately from January through October with a tendency to dissipate or change sign around November. Changes of the Indonesian SST anomaly lead by about a season changes in the Southern Oscillation and the eastern Pacific SST anomaly.

Allan and Pariwono (1990) studied the ocean-atmosphere couplings in low-latitudes of the Australian-Asian region (Australasia) through an examination of the relative importance of wind-stress-SST mechanisms, cloudiness-radiation mechanisms, and the possible influence of SST advection, oceanic mixing, the Indonesian throughflow, and low-level forcings during anti-ENSO and ENSO events. The anti-ENSO (ENSO) events are marked by easterly (westerly) wind-stress anomalies in the western equatorial Pacific, southerly (northerly) wind-stress anomalies in the eastern Indonesian and eastern Coral Sea regions, positive (negative) SST anomalies and weak (strong) SST advection in northern Australian waters, positive (negative) cloudiness anomalies over Australasia and high (low) sea-level anomalies at southern Philippines and northern Australia. However, there seems to be no conclusive evidence for the influence of oceanic throughflow on ocean-atmosphere interactions, and thus anti-ENSO and ENSO phases. Nevertheless, there are indications that the Indonesian throughflow is modulated by remote low-frequency forcings of the tropical variability.

The extensive description, dynamics, and role of the Indonesian throughflow have been presented in a special issue of the *Journal of Geophysical Research* in 1996. Meyers (1996) found the net transport from the Pacific Ocean to the Indian Ocean is a maximum during the 1988/89 La Niña event and minimum during the 1986/87 and 1991/94 El Niño

events. Bray et al. (1996) explained the thermocline depth changes at the Timor Sea and the Flores Sea at interannual time scales appear to be related with sea level and SOI fluctuations. During ENSO events, sea level drops and thermocline rises.

On the annual variations, Godfrey (1996) gave estimates of the Indonesian throughflow transport that vary from essentially nil to 20 Sv. Meanwhile, Masumaoto and Yamagata (1996) showed an annual mean transport of 9.5 Sv from the Pacific to the Indian oceans with a maximum (minimum) transport of 11.6 Sv (6.0 Sv) in August (July).

The role of the Indonesian throughflow in the global climate system is investigated by Schnider (1998). An open throughflow increases surface temperatures in the eastern Indian Ocean, reduces temperatures in the equatorial Pacific, and shifts the warm pool and centers of deep convection in the atmosphere to the west. This control on SST and deep convection affects atmospheric pressure in the entire tropics and, via atmospheric teleconnections, in the midlatitudes. As a result, surface wind-stress in the entire tropics changes and the meridional and zonal gradients of the tropical thermocline and associated currents increase in the Pacific Ocean and decrease in the Indian Ocean. The response includes an acceleration of the equatorial undercurrent in the Pacific Ocean, and a deceleration in the Indian Ocean. Thus, the Indian throughflow exerts significant control over the global climate in general, and the tropical climate in particular.

2.3.2 Over the Indian Ocean

The Indian Ocean is the third largest body of water in the world covering about 20% of the earth's water surface. Its climate system has vital social and economic consequences

particularly for population over the Asian-Australian region. The ITCZ over the Indian Ocean during the northeast monsoon episode is strongly determined by planetary-scale processes such as the large-scale heating over the northeast Australia, the monsoon trough, and warm SST. In addition, the SST distribution and the eastward 30-50 day oscillation are important processes that modulate the northeast monsoon variability over the Indian Ocean.

Recent observations and modeling effort over the Indian Ocean have been focused on the predictability of the monsoon climate system and its role on the predictability of the global climate system in particular that related to ENSO. Latief et al. (1994) simulated seasonal and interannual variability of the tropical Indian Ocean using the coupled GCM. Their study showed the annual cycle of SST and rainfall are realistically simulated. The amplitudes of the seasonal changes, however, are underestimated. The model also simulates considerable interannual variability in the tropical Indian Ocean circulation. Changes in the surface wind-stress appear to be crucial in forcing the interannual variations in the Indian Ocean SST. However, the model fails to simulate sufficient interannual variability in monsoon rainfall due to incorrect simulation in SST anomalies.

Nagai et al. (1995) examined the atmosphere-ocean interaction of ENSO with and without an active Indian Ocean by comparing two coupled GCM models: one is having the tropical Pacific as the ocean model domain (PAC), and the other is having the tropical Pacific and Indian oceans as the ocean model domain (IPC). Both models have succeeded in simulating reasonably realistic ENSO phenomena. This implies that ENSO is fundamentally the oscillatory phenomena in the Pacific basin and that the Indian Ocean

does not play any active role in the ENSO dynamics. On the other hand, interannual variability of monsoon activity in the IPC model is more reasonable than that in the PAC model.

Gautier et al. (1998) used the multispectral satellite data to investigate the spatial and temporal variability of air-sea interactions over the Indian Ocean. Significant negative correlations between precipitation and the net surface solar short-wave radiation (SW) are observed over most of the northern Indian Ocean indicating that an increase (decrease) in precipitation is associated with a decrease (increase) in SW. On the other hand, the negative correlations between precipitation and the latent heat flux (LHF) are found south of 10°S arising primarily from the seasonal cycle. Furthermore, strong annual variations in precipitation and SST are observed over the Arabian Sea and the Bay of Bengal. Precipitation variations are much stronger over the Bay of Bengal than over the Arabian Sea which are consistent with other studies (e. g., Mohanty et al. 1994). On the interannual time scales, positive anomalies in precipitation are observed throughout the Arabian Sea in summer 1988 during La Niña event. Accordingly, strong negative anomalies of SW occurred across the entire Arabian Sea and positive anomalies of LHF occurred over the southern Indian Ocean.

Webster et al. (1998) explained how El Niño imparts an influence on the Indian Ocean. During a normal period (Fig. 2.7a), precipitation occurs over Indonesia and the warm pool associated with lower tropospheric wind convergence of the Walker circulation. These converging winds provide an eastward wind-stress over the Pacific Ocean and a westward stress over the Indian Ocean, tilting each ocean upwards towards Indonesia and flanking the archipelago with deep warm mixed layers. The subsiding of

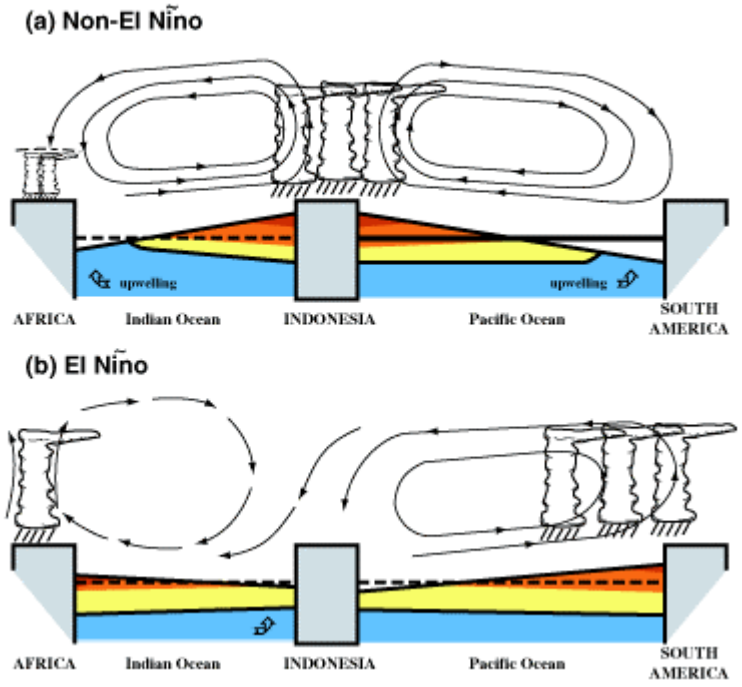

Figure 2.7. Schematic diagram of the large-scale differences along the equatorial Pacific and Indian oceans between a) normal periods and b) El Niño periods. Adapted from Webster et al. (1998).

the Walker circulation inhibits precipitation in the eastern Pacific Ocean and western Indian Ocean. With the advent of El Niño (Fig. 2.7b), the eastward migration of the Walker circulation increases subsidence over Indonesia. Over East Africa, the subsidence is reduced and deep convection forms over the heated continent which, in turn, causes inflow into Africa from the Indian Ocean where the wind-stress is reversed, flattening the ocean surface or even tilting it slightly upward towards the west. The subsequent deepening of the mixed layer in the western Indian Ocean reduces the mixing of old

water from below and helps maintain the warm SST anomaly throughout the El Niño event.

A comprehensive research data set collected during the Indian Ocean Experiment (INDOEX) from 1996 to 1999 provides a valuable research on the ITCZ dynamics. The equatorial Indian Ocean during the northeast monsoon episode is a unique natural laboratory and the only place in the world where an intense source of continental aerosol, anthropogenic trace species, and their reaction products (e. g., sulfate and ozone) from the Northern Hemisphere are directly connected to the pristine air of the Southern Hemisphere by a cross equatorial monsoonal flow into the ITCZ. Furthermore, the deep convection within the ITCZ gives rise to extensive mid- and upper-level cloud systems.

INDOEX is an international field experiment with the following primary objectives (*http://www-indoex.ucsd.edu*):

a. asses the significance of sulfates and other continental aerosols for global radiative forcings.
b. asses the magnitude of the solar absorption at the surface and in the troposphere including the ITCZ cloud systems.
c. asses the role of the ITCZ in the transport of trace species and pollutants and their resultant radiative forcing.

The special INDOEX composite observing systems such as four US aircraft, a Dutch aircraft, a German research vessel, a German and an Indian research vessels, French constant level balloons, two island stations, operational and research satellites, and four-dimensional high resolution analyzed fields have been used for addressing these objectives.

During the six week field experiment in February-March 1999, the INDOEX scientists reported finding a dense, brown haze of pollution extending from the ocean surface to altitudes of 1-3 km (*News and Notes, Bull. Amer. Meteor. Soc., 8, 1729-1732*). The haze layer covers much of the research area almost continually during this period. The affected area includes most of the northern Indian Ocean, including the Arabian Sea, much of the Bay of Bengal, and spills over into the equatorial Indian Ocean at about 5°S. Asia and the Indian subcontinent, which have a population of more than two billion, emit large quantities of pollutants that can be carried to the Indian Ocean during the northeast monsoon. Preliminary results indicate that aerosols in the polluted region scatter the incoming solar radiation and reduce the amount of energy absorbed by the ocean surface by as much as 10%.

The dark airborne particles over the Indian Ocean appear to be markedly different from those over North America and Europe, where advanced pollution control technologies remove much of the dark material and yield particles that are relatively brighter. Thus, the impact on climate processes of pollution particles stemming from Asia appears to be fundamentally different from those originating in the United States and Europe. The measurements taken in the Indian Ocean are also important because they characterize emissions from rapidly emerging economies in this region.